Hindawi
Mathematical Problems in Engineering
Volume 2019, Article ID 1683989, 9 pages
https://doi.org/10.1155/2019/1683989

Research Article

Production Decline Behavior Analysis of a Vertical Well with a Natural Water Influx/Waterflood

Mingqiang Wei,[1] **Keyi Ren**,[1] **Yonggang Duan**,[1] **Qingxuan Chen**,[2] **and Morteza Dejam**[3]

[1]*State Key Laboratory of Oil and Gas Reservoir Geology and Exploitation, Southwest Petroleum University, Chengdu 610500, Sichuan, China*
[2]*3rd Gas Production Plant, PetroChina Changqing Oil Field Branch, Uxin Banner 017300, Inner Mongolia, China*
[3]*Department of Petroleum Engineering, College of Engineering and Applied Science, University of Wyoming, 1000 East University Avenue, Laramie, WY 82071-2000, USA*

Correspondence should be addressed to Yonggang Duan; nanchongdyg@163.com

Received 11 April 2019; Accepted 13 August 2019; Published 2 September 2019

Academic Editor: Dragan Poljak

The production decline type curves are considered as a robust technique to interpret the production data and obtain the flow parameters, the original gas in place, etc. However, most of the previous models have focused on the primary depletion with a closed boundary, rather than on the secondary depletion with a water influx/waterflood. Therefore, in this study, a transient flow model considering the water influx/waterflood is developed. Subsequently, the functions of the production decline type curves for a vertical well with a water influx/waterflood are derived based on the material balance equation. In other words, the theory of Blasingame production decline analysis is extended to the water influx/waterflood reservoir. Further advanced Blasingame production decline type curves for a vertical well in water influx/waterflood reservoirs are generated. Compared with Blasingame type curves without a water influx/waterflood, the behavior of the ones presented in this study is quite different at the boundary. Thereafter, the effects of the relevant parameters, including the dimensionless maximum water influx, the dimensionless beginning time of the water influx, and the dimensionless external boundary radius, are studied on type curves. Finally, Blasingame type curves for a vertical well in water influx/waterflood reservoirs are verified through a field case study. This work provides very meaningful references for reservoir engineers working on the evaluation of the water influx and the estimation of the beginning time of the water influx by matching the developed type curves with the actual field data.

1. Introduction

There are many water influx gas reservoirs in the world, such as Longwangmiao gas reservoir [1], California Monterey reservoir [2], and Baiyun sag reservoir in the Pearl River Mouth Basin [3]. The water influx has a significant effect on the gas well production. Therefore, the diagnosis and evaluation of the water influx rate and the water influx time are vital in exploitation of these reservoirs.

Over the past decades, the production performance behavior for a vertical well in water influx/waterflood reservoirs has been studied analytically, semianalytically, and numerically. Van Everdingen and Hurst [4], Fetkovich [5], Carter and Tracy [6], Allard and Chen [7], Leung [8], and Shen et al. [9, 10] developed mathematical models for evaluation of the aquifer properties. Subsequently, Marques and Trevisan [11] compared the simulation results for four classical water influx models [4–6, 8] and discussed the applicable conditions for these models. Based on the two-phase unsteady flow theory, Cui and Zhao [12] presented a technique for calculating production index in multilayer water-drive reservoirs. Later, Omeke et al. [13] developed a new aquifer influx model for a finite aquifer system in order to describe the pseudosteady flow regime. The proposed prediction model was fast and the obtained results showed a reasonable degree of accuracy. Thereafter, Li et al. [14] presented a method for identification and prediction of water influx in a fractured-vuggy carbonate reservoir. The

four diagnostic curves for identifying aquifer influx phase were proposed.

Although the previous proposed models can be used for forecasting the production in water influx reservoirs, they have not taken the effect of material balance into account. Among the transient analysis models [15–17] and production analysis methods [18–23], the Blasingame type curves technique [21–23] derived using the reservoirs' material balance equation is a very popular and practical production decline analysis. This method, which can be used to evaluate the reservoir properties, drainage volume, etc., has been widely implemented in conventional reservoirs for several decades. However, most of the previous efforts [22, 24–28] for improving the Blasingame decline type curves analysis have been mainly focused on the primary production, rather than on the secondary depletion.

Considering the effect of water influx/waterflood, Doublet and Blasingame [29] proposed the model of Fetkovich decline analysis and generated the Fetkovich decline type curves. However, this model, which is based on highly idealized assumed production conditions, cannot be used to analyze the various production scenarios (including different rates and various flowing pressures). Until now, the works that have extended the Blasingame decline type curves for analyzing water influx data are limited. Therefore, the aim of this work is to study the Blasingame production decline type curves behavior for a vertical well with a water influx/waterflood.

In this study, first, the transient flow model is developed considering the water influx/waterflood with a ramp rate at the external boundary. Then, the functions of the Blasingame decline type curves for a vertical well with a water influx/waterflood are derived. In other words, the theory of Blasingame production decline analysis is generalized to the water influx/waterflood reservoir. Subsequently, Blasingame production decline type curves are generated. The four flow regimes, including early unsteady flow regime, primary depletion flow regime, second unsteady flow regime, and system pseudosteady flow regime, are recognized. In addition, the effects of relevant parameters such as the dimensionless maximum water influx, the dimensionless beginning time of the water influx, and the dimensionless external boundary radius are studied on the type curves. Finally, type curves are verified through a field case study. This study can provide very meaningful references for reservoir engineers in water influx rate evaluation as well as the beginning time of the water influx estimation by matching the type curves with the actual field data.

2. Mathematical Model with a Natural Water Influx/Waterflood

2.1. Physical Model and Its Assumptions. The physical model with a water influx/waterflood at the external boundary is shown in Figure 1. The model under study assumes that a vertical well is centered in a bounded circular reservoir with a constant rate at the inner boundary and water influx at the outer boundary. The other basic assumptions of the model are as follows:

(1) The reservoir is homogenous, anisotropic, and horizontal with closed top and bottom boundaries. The characteristic parameters (such as thickness, permeability, porosity, and initial pressure) of the reservoir are constant.

(2) The fluid is considered as a single phase. The other properties of the fluid remain constant.

(3) The fluid flow follows Darcy's law. The well produces gas at a constant rate.

(4) The influx at the outer boundary is initially zero and the water influx gradually increases from zero at the initial time to a fixed value at a certain time. The waterflood case is named as the "ramp" rate case by Doublet and Blasingame [29].

(5) The reservoir is isothermal and the effect of gas gravity is neglected.

2.2. Mathematical Model and Its Solution. Based on the above assumptions, the partial differential equation describing the fluid flow can be derived in terms of pseudopressure as follows:

$$\frac{\partial^2 \psi}{\partial r^2} + \frac{1}{r}\frac{\partial \psi}{\partial r} = \frac{\mu \phi c_t}{k}\frac{\partial \psi}{\partial t}, \tag{1}$$

where r is the radius distance from the wellbore (m), ψ is the reservoir pseudopressure (MPa^2/MPa·s), k is the permeability (10^{-3} μm^2), ϕ is the porosity (decimal), μ is the fluid viscosity (MPa·s), c_t is the total compressibility (MPa^{-1}), and t is the time (day).

The definition of the pseudopressure is

$$\psi = 2\int_{p_0}^{p} \frac{p}{\mu z}\, dp. \tag{2}$$

Initial boundary condition:

$$\psi(r, 0) = \psi_i. \tag{3}$$

Internal (or inner) boundary condition:

$$\frac{2\pi kh}{\mu B}\left(r\frac{\partial \psi}{\partial r}\right)_{r=r_w} = q. \tag{4}$$

External (or outer) boundary condition:

$$\frac{2\pi kh}{\mu B}\left(r\frac{\partial \psi}{\partial r}\right)_{r=r_e} = q_{ext}(t), \tag{5}$$

where ψ_i is the initial pseudopressure (MPa^2/MPa·s), r_w is the well radius (m), h is the thickness of the pay zone (m), q is the production per day (m^3/d), B is the fluid formation volume factor (decimal), r_e is the radius distance of the external boundary at the water influx (m), and $q_{ext}(t)$ is the water influx at the external boundary (m^3/day), which is a function of the time.

Doublet and Blasingame [29] proposed the "Ramp" waterflood flux function as follows:

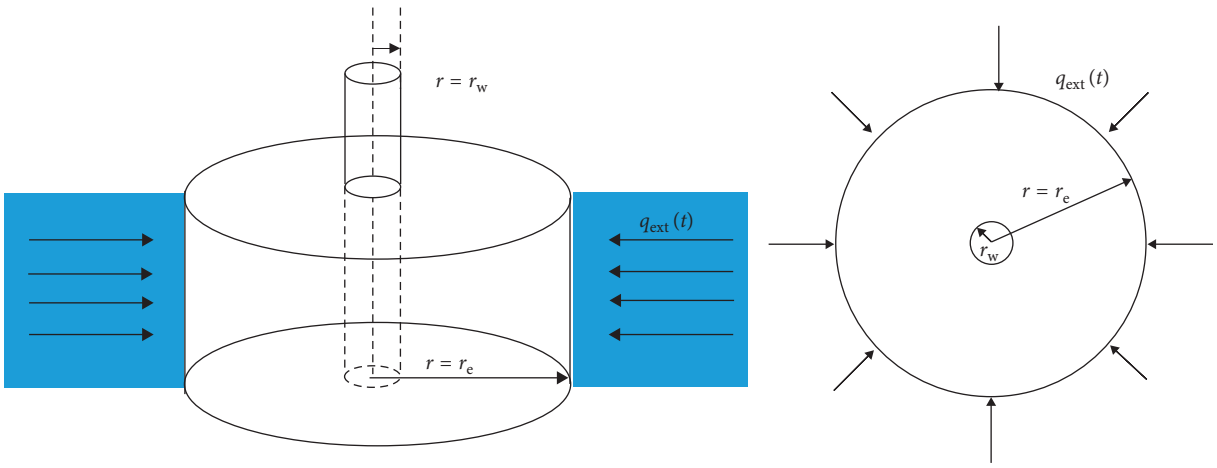

FIGURE 1: Physical model of the water-drive reservoir. r is the radial radius, r_w is the well radius, r_e is the radius distance of the external boundary at the water influx, and $q_{ext}(t)$ is the water influx at the external boundary.

$$q_{ext}(t) = q_{ext,\infty}\left[1 - \exp\left(\frac{-t}{t_{start}}\right)\right], \tag{6}$$

where t_{start} is the beginning time of the water influx (day) and $q_{ext,\infty}$ is the maximum water influx, which does not exceed the well production (m^3/d).

To simplify the derivation of equations, first, the dimensionless definition of all the variables (listed in Table 1) used in the proposed mathematical model is presented.

Using the formula of the dimensionless waterflood flux at the external boundary in Table 1, the dimensionless "Ramp" waterflood fluxes at the external boundary with different $q_{Dext,\infty}$ and t_{Dstart} are shown in Figures 2 and 3, respectively. As $q_{Dext,\infty}$ increases, the values of q_{Dext} become larger after t_{Dstart} (Figure 2). The values of q_{Dext} increase with increasing t_{Dstart}, but finally, the q_{Dext} curves converge into one horizontal line (Figure 3). Consequently, $q_{Dext,\infty}$ and t_{Dstart} have significant effects on the production decline behavior of the natural water influx reservoirs or the artificial waterflood reservoirs.

Based on the definition of all the dimensionless variables listed in Table 1, equations (1) and (3)–(5) of the mathematical model can be converted and written in the following dimensionless forms:

$$\frac{1}{r_D}\frac{\partial}{\partial r_D}\left[r_D\frac{\partial \psi_D}{\partial r_D}\right] = \frac{\partial^2 \psi_D}{\partial r_D^2} + \frac{1}{r_D}\frac{\partial \psi_D}{\partial r_D} = \frac{\partial \psi_D}{\partial t_D}, \tag{7}$$

$$\psi_D(r_D, t_D = 0) = 0, \tag{8}$$

$$\left[r_D\frac{\partial \psi_D}{\partial r_D}\right]_{r_D=1} = -1, \tag{9}$$

$$\left[r_D\frac{\partial \psi_D}{\partial r_D}\right]_{r_D=r_{eD}} = q_{Dext}(t_D). \tag{10}$$

TABLE 1: Dimensionless definition of all the variables used in this study.

Dimensionless pressure	$\psi_D = (kh/q\mu B)\Delta\psi$
Dimensionless radius	$r_D = r/r_w$
Dimensionless radius at the external boundary	$r_{eD} = r_e/r_w$
Dimensionless maximum water influx	$q_{Dext,\infty} = q_{ext,\infty}/q$
Dimensionless time	$t_D = kt/\mu\varphi c_t r_w^2$
Dimensionless waterflood flux at the external boundary	$q_{Dext}(t_D) = q_{Dext,\infty}[1 - \exp(-t_D/t_{Dstart})]$

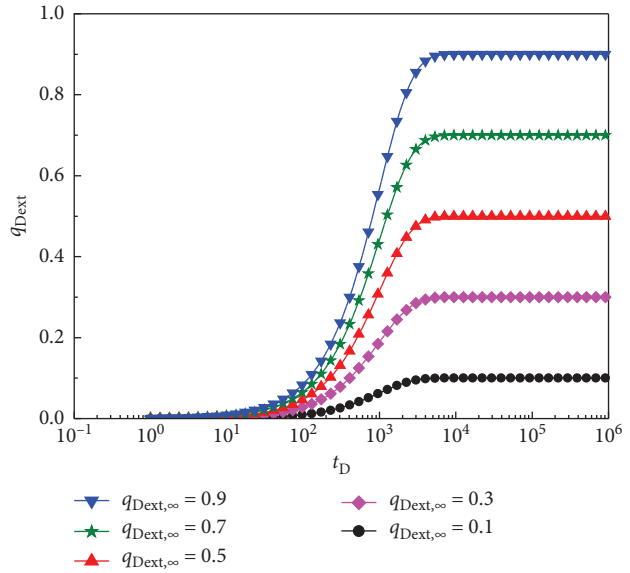

FIGURE 2: The dimensionless "Ramp" waterflood flux at the external boundary versus the dimensionless time for $t_{startD} = 10^3$.

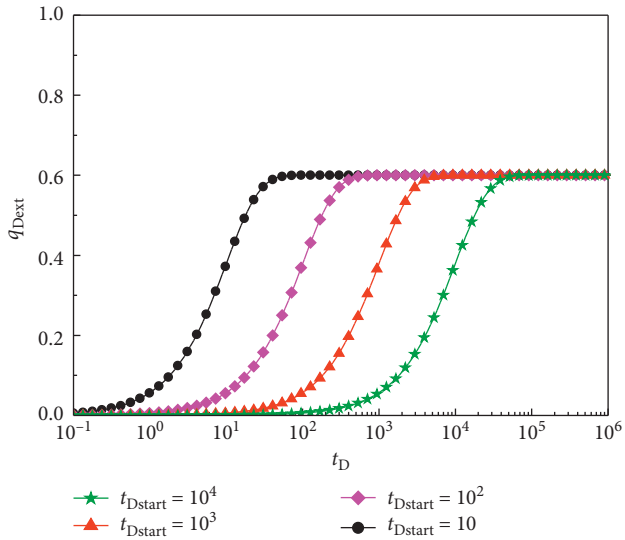

FIGURE 3: Schematic of the dimensionless "Ramp" waterflood flux at the external boundary versus the dimensionless time with $q_{Dext,\infty} = 0.6$.

To solve the equations, the mathematical model is first transformed into Laplace domain. With Laplace transformation, equations (7)–(10) can be written as

$$\frac{1}{r_D}\frac{\partial}{\partial r_D}\left[r_D\frac{\partial \overline{\psi}_D}{\partial r_D}\right] = s\overline{\psi}_D, \tag{11}$$

$$\overline{\psi}_D(r_D, t_D = 0) = 0, \tag{12}$$

$$\left[r_D\frac{d\overline{\psi}_D}{dr_D}\right]_{r_D=1} = -\frac{1}{s}, \tag{13}$$

$$r_D\frac{d\,\overline{\psi}_D}{dr_D}\bigg|_{r_D=r_{eD}} = \overline{q}_{Dext}(s). \tag{14}$$

Combining equations (11)–(14), the pressure response solution of equation (11) can be obtained as follows [29]:

$$\overline{\psi}_D(r_D = 1, s) = \frac{1}{s\sqrt{s}}\frac{K_0(\sqrt{s})I_1(r_{eD}\sqrt{s}) + K_1(r_{eD}\sqrt{s})I_0(\sqrt{s})}{K_1(\sqrt{s})I_1(r_{eD}\sqrt{s}) - K_1(r_{eD}\sqrt{s})I_1(\sqrt{s})} + \frac{\overline{q}_{Dext}(s)}{\sqrt{s}r_{eD}}\frac{K_0(\sqrt{s})I_1(\sqrt{s}) + I_0(\sqrt{s})K_1(\sqrt{s})}{K_1(\sqrt{s})I_1(r_{eD}\sqrt{s}) - K_1(r_{eD}\sqrt{s})I_1(\sqrt{s})}, \tag{15}$$

where $K_0(x)$ is the modified Bessel function of second kind (zero order), $K_1(x)$ is the modified Bessel function of second kind (first order), $I_0(x)$ is the modified Bessel function of first kind (zero order), and $I_1(x)$ is the modified Bessel function of first kind (first order).

In equation (15), the first part is the "no-flow" boundary solution and the second part is the boundary flux solution [29]. In addition, the transient pressure solution for a vertical well in a natural water influx/waterflood homogenous reservoir can be generalized to a fractured natural water influx/waterflood reservoir and different well configurations.

3. Production Decline Analysis Theory

The dimensionless pressure solution in the Laplace domain can be obtained using the dimensionless rate solution, as proposed by Van Everdingen and Hurst [4]:

$$q_D(s) = \frac{1}{s^2}\frac{1}{\overline{\psi}_D(s)}. \tag{16}$$

The subject of the production performance behavior of the natural water influx/waterflood reservoirs is significant because the water invasion has an important effect on the well production. On the other side, the water invasion behavior and water influx rate are difficult to diagnose by the dynamic monitoring technology. The response of transient production decline type curves for conventional primary depletion reservoirs with a closed boundary were presented in the works performed by Palacio and Blasingame [21]; Doublet et al. [29] and Marhaendrajana and Blasingame [30]. This section generalizes the Blasingame transient production decline type curves to a new reservoir model with a "ramp" boundary flux for the water influx reservoirs.

3.1. Material Balance Equation for Natural Water Influx/Waterflood Reservoirs. The material balance equation is the theoretical basis of the Blasingame decline type curves. However, the material balance equation of traditional closed boundary reservoirs is not appropriate for natural water influx/waterflood reservoirs. The material balance equation of water influx/waterflood reservoirs can be derived as follows:

$$G_pB_g + W_pB_w = G\left(B_g - B_{gi}\right) + GB_{gi}\left(\frac{c_ws_{wi} + c_f}{1 - s_{wi}}\right)(p_i - p) + W_e, \tag{17}$$

where G is the reserve of the natural water influx/waterflood reservoir; G_p and W_p are the productions of the gas and water, respectively; W_e is the water influx rate; c_g, c_w, and c_f are the compressibilities of the gas, water, and rock, respectively; s_{wi} is the irreducible water saturation; p is the reservoir pressure; B_g and B_{gi} are the gas volume coefficients at the pressure p and the initial reservoir pressure p_i, respectively; and B_w is the water volume coefficient.

To facilitate the derivation of equation (17), the volume coefficient of the water, M, is defined as the ratio between water volume and pore volume in the reservoir:

$$M = \frac{V_{wi}}{\left(GB_{gi}/1 - S_{wi}\right)}, \tag{18}$$

where V_{wi} is the water volume in the reservoir.

Considering the effect of the water expansion and the shrinkage of the rock, the expression of the water influx can be written as

$$W_e = V_{wi}(c_f + c_w)\Delta p = M\frac{NB_{gi}\Delta p}{1 - s_{wi}}(c_f + c_w), \tag{19}$$

where Δp is the pressure drop from pressure p_i to pressure p.

Inserting equation (19) and the real gas state equation into equation (16), one can reach to

$$\frac{p}{z}\left\{1 - \left[\frac{c_w s_{wi} + c_f + M(c_f + c_w)}{1 - s_{wi}}\right]\Delta p\right\} = \frac{p_i}{z_i}\left(1 - \frac{Q_p}{G}\right), \tag{20}$$

where z_i and z are the deviation factors at the initial reservoir pressure p_i and the pressure p, respectively, and Q_p is the pseudocumulative production rate, which is defined as follows:

$$Q_p = G_p + \frac{W_p B_w}{B_g}. \tag{21}$$

3.2. Blasingame Production Decline Analysis Theory. To simplify equation (20), a new parameter (c_a) is defined as follows:

$$c_a = \frac{c_w s_{wi} + c_f + M(c_f + c_w)}{1 - s_{wi}}. \tag{22}$$

Taking the derivative of equation (20) with respect to t gives

$$\frac{dp}{dt} = -\frac{p_i q_p}{z_i G}\frac{z(1 - s_{wi})}{p\left\{\left[(M + s_{wi})c_w + (M + 1)c_f + (1 - s_{wi})c_g\right] - (\partial c_d/\partial p)\right\}}, \tag{23}$$

where c_g is the gas compressibility and q_p is the pseudoproduction rate, which is defined as follows:

$$q_p = \frac{dQ_p}{dt}. \tag{24}$$

In equation (23), $\partial c_d/\partial p$ can be derived as

$$\frac{\partial c_d}{\partial p} = c_g\left[(M + s_{wi})c_w + (M + 1)c_f\right](p_i - p). \tag{25}$$

In order to simplify equation (23), the total compressibility c_t is defined as

$$c_t = \frac{\left[(M + s_{wi})c_w + (M + 1)c_f + (1 - s_{wi})c_g\right] - (\partial c_d/\partial p)}{1 - s_{wi}}. \tag{26}$$

Combining equations (23), (25), and (26), the flow production equation in the natural water influx/waterflood reservoir can be obtained as follows:

$$q_p = -\frac{z_i G c_t p}{z p_i}\frac{dp}{dt}. \tag{27}$$

Additionally, to analyze the case of the variable rate/pressure data for a gas well, Palacio and Blasingame [21] introduced the material balance pseudotime function for a gas well and proposed the Blasingame production decline type curves analysis method.

The material balance pseudotime function is

$$t_{ca} = \frac{(\mu C_t)_i}{q}\int_0^t \frac{q}{\mu C_t}dt. \tag{28}$$

Inserting equation (27) into equation (28), the material balance pseudotime equation can be rewritten as

$$t_{ca} = \frac{(\mu c_t)_i}{q}\int_{p_i}^{p}\frac{z_i G p}{z p_i \mu}dp = \frac{G(\mu c_t z)_i}{q p_i}\int_{p_i}^{p}\frac{p}{\mu z}dp. \tag{29}$$

To simplify equation (29), the normalized pseudopressure is defined as below:

$$p_p = \left(\frac{\mu_g z}{p}\right)_i\int_0^p \frac{p}{\mu_g z}dp. \tag{30}$$

In addition, taking equation (30) into equation (29), the material balance pseudotime equation can be rewritten as

$$t_{ca} = \frac{G c_{ti}}{q}(p_{pi} - p_p), \tag{31}$$

where p_{pi} and p_p are the normalized pseudoinitial reservoir pressure and normalized pseudoreservoir pressure, respectively.

According to the flow theory in porous media, the standard pseudosteady flow equation can be written as follows:

$$q = J\lfloor p_p - p_{pwf}\rfloor, \tag{32}$$

where J is the gas production index.

Combining equations (31) and (32) results in

$$\frac{p_{pi} - p_{Pwf}}{q} = m_a t_{ca} + b_{a,pss}, \tag{33}$$

where $m_a = 1/(G \times c_{ti})$ and $b_{a,pss} = (\mu \times z)_i/(2 \times J \times p_i)$.

Equation (33) in water influx reservoirs is consistent with the one in dry gas reservoirs. Therefore, the model proposed above can be extended to water influx reservoirs.

Based on the above similar theory derivation, Palacio and Blasingame [20] developed the theory of Blasingame production decline type curves analysis. These Blasingame decline type curves are summarized in Table 2.

The production decline type curves are generally defined using the following dimensionless parameters [20, 30].

Dimensionless normalized production function:

$$q_{Dd} = \frac{b_{a,pss}}{\Delta p_p}t_{ca} = q_D\left[\ln r_{eD} - \frac{1}{2}\right]. \tag{34}$$

Dimensionless material balance pseudotime:

$$t_{Dd} == \frac{m_a}{b_{a,pss}}\frac{2}{r_{eD}^2}\frac{1}{[\ln r_{eD} - (1/2)]}t_D. \tag{35}$$

Dimensionless normalized cumulative production integral function:

$$q_{Ddi} = \frac{1}{t_{Dd}}\int_0^{t_{Dd}} q_{Dd}(\tau)d\tau. \tag{36}$$

Dimensionless production integral derivative function:

Table 2: Summary of the Blasingame decline type curves.

Case	Plotting function
Dimensionless normalized production curve	q_{Dd} versus t_{Dd}
Dimensionless normalized cumulative production integral curve	q_{Ddi} versus t_{Dd}
Dimensionless production integral derivative curve	q_{Ddid} versus t_{Dd}

$$q_{Ddid} = -\frac{dq_{Ddi}}{d\ln t_{Dd}} = -t_{Dd}\frac{dq_{Ddi}}{t_{Dd}}. \quad (37)$$

4. Results and Discussion

4.1. Model Validation and Comparison. According to the above production decline analysis theory, the Blasingame type curves can be obtained by using one of the numerical Laplace inversion methods, including Stehfest, Zakian, Fourier series, and Schapery methods [31–33]. Here, the Stehfest method is applied [34]. For this study, if the water influx/waterflood at the external boundary, $q_{Dext,\infty}$, is equal to zero, the proposed model can be reduced to the traditional closed boundary model.

Figure 4 shows the type curves for a vertical well with a traditional closed boundary model and water influx/waterflood $q_{Dext,\infty} = 0.7$ at the external boundary model. From Figure 4, it can be observed that the rate decline curves behavior is quite different in the boundary response regime. The slope of the dimensionless normalized production curve is −1 (angle = 45°) in the pseudosteady flow regime dominated by the closed boundary, whereas the slope of the dimensionless normalized production curve is not equal to −1 in the regimes dominated by the water influx/waterflood boundary.

In addition, according to the behavior of the Blasingame production decline curves (Figure 5), type curves can be divided into the four regimes: (I) early unsteady flow regime (EUFR) around the vertical well, which represents the pressure wave spreads continuously away from the wellbore; (II) the primary depletion flow regime (PDFR); (III) the second unsteady flow regime (SUFR) resulting from the external pressure support such as natural water influx or waterflood; and (IV) system pseudosteady flow regime (SPSF), in which dimensionless normalized production curve has a slope of −1 (angle = 45°).

4.2. Sensitivity Analysis. Most of the previous studies have focused on the closed boundary model, rather than on the natural water influx or waterflood model at the external boundary. Thus, the sensitivity of relevant parameters of the water influx or waterflood is discussed in detail in this section.

Figure 6 shows that the dimensionless maximum water influx has a significant effect on the second unsteady flow regime and system pseudosteady flow regime. From Figure 6, it can be observed that the greater the dimensionless maximum water influx, the larger the values of q_{Dd}, q_{Ddi}, and

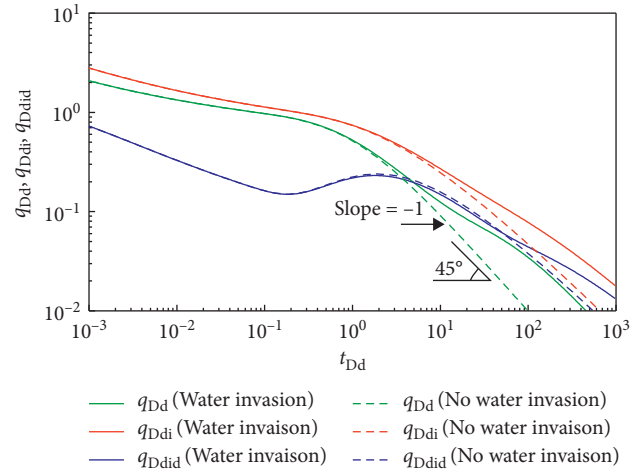

Figure 4: Comparison of Blasingame type curves with different boundary models.

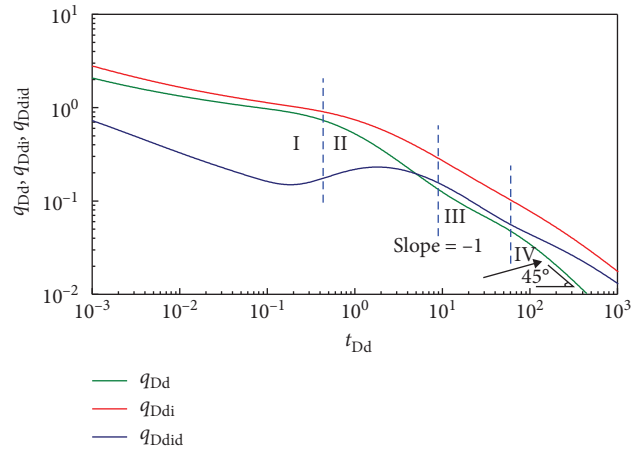

Figure 5: Blasingame production decline type curves by considering natural water influx or waterflood.

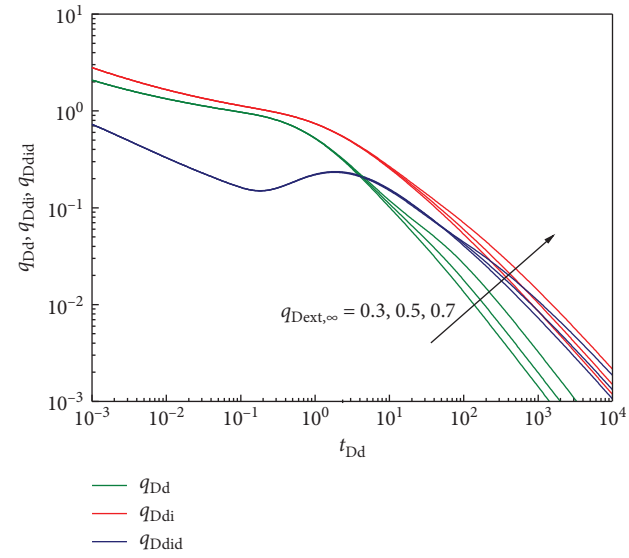

Figure 6: Effect of the dimensionless maximum water influx ($q_{Dext,\infty}$) on type curves.

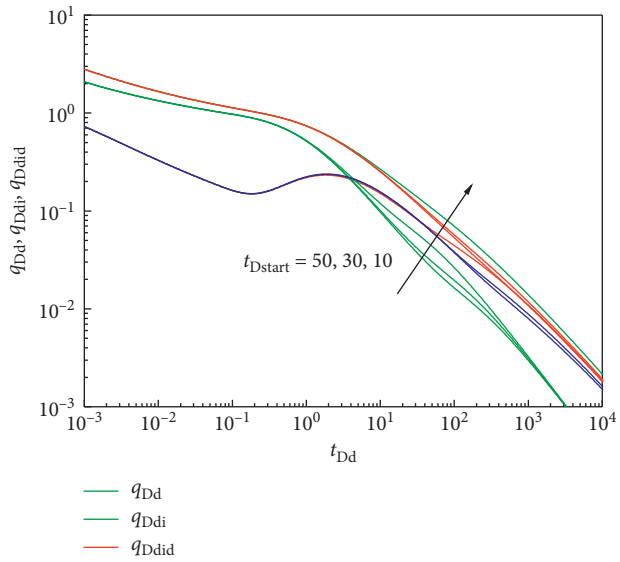

Figure 7: Effect of the dimensionless beginning time of the water influx (t_{Dstart}) on type curves.

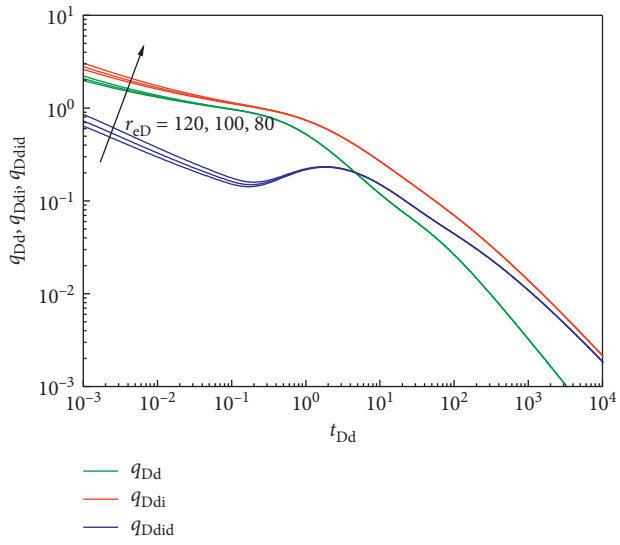

Figure 8: Effect of the dimensionless external boundary radius (r_{eD}) on type curves.

q_{Ddid} for the type curves happen during the second unsteady flow regime and system pseudosteady flow regimes. The main reason is that the external pressure support of the natural water influx or waterflood becomes greater with an increase in the dimensionless maximum water influx.

Figure 7 illustrates the effect of the dimensionless beginning time of the water influx (t_{Dstart}) on the second unsteady flow regime of the Blasingame production decline type curves. As t_{Dstart} increases, the regime of the second unsteady flow emerges earlier. According to the emerging time of the second unsteady flow regime, the type curves can be used to estimate the t_{Dstart} by type curve history matching.

Figure 8 shows the effect of the dimensionless external boundary radius (r_{eD}) on production decline type curves. It

Table 3: Basic parameters for the production decline analysis.

Parameters	Unit	Value
Well radius, r_w	m	0.1
Thickness of the pay zone, h	m	18
Reservoir porosity, ϕ	Decimal	0.253
Initial reservoir pressure, p_i	MPa	14.6
Reservoir temperature, T	°C	80
Gas gravity, r_g	Decimal	0.57
Initial water saturation, s_{wi}	Decimal	0.25
Rock compressibility, c_f	MPa^{-1}	5.55×10^{-4}
Water compressibility, c_w	MPa^{-1}	4.67×10^{-4}
Gas compressibility, c_g	MPa^{-1}	7.12×10^{-4}

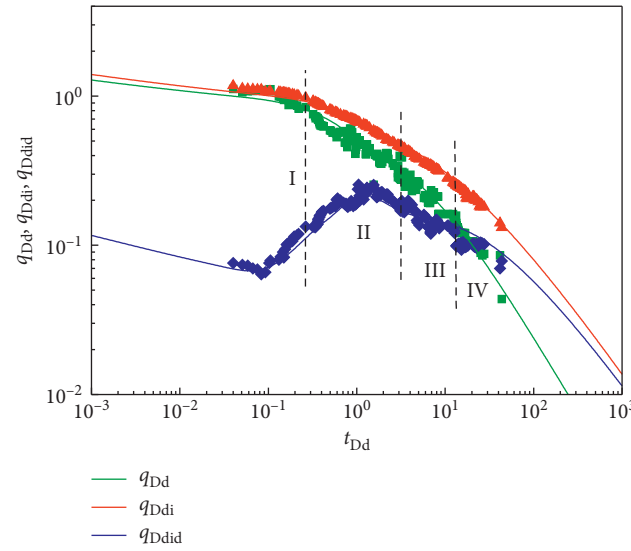

Figure 9: The matched curves of the Blasingame production decline for well A1.

can be observed that first regime are governed by r_{eD}. As the dimensionless external boundary radius increases, the values of q_{Dd}, q_{Ddi}, and q_{Ddid} for the type curves become smaller during the early unsteady flow regime. According to the early unsteady flow regime behavior of the Blasingame decline type curves, the type curves can be used to estimate the r_{eD} by type curves history matching.

5. Field Application

A field case is presented to demonstrate the application of the model proposed in this study. Well A1 is located in an offshore sand reservoir in the western South China Sea. The reservoir is a typical gas reservoir driven by the edge water. The basic parameters for the production decline analysis are given in Table 3.

The production data of well A1 are matched and analyzed by the Blasingame production decline analysis technique with the water influx/waterflood model. Figure 9 shows that the Blasingame production decline type curves match the real production data well. On the other hand, the behavior of type curves of water invasion (regime III and regime IV) can be observed clearly from Figure 9. The

Table 4: Results of the Blasingame production decline analysis for well A1.

Parameters	Unit	Value
Permeability, k	mD	10.9
Distance from the well to the circular boundary, r_e	m	76.32
Maximum water influx, $q_{Dext,\infty}$	Decimal	0.86
Beginning time of the water influx, t_{Dstart}	Decimal	1.52
Volume coefficient of water, M	Decimal	0.25
Well's original gas in place, N_v	$10^8\,m^3$	7.62

relevant parameters (Table 4) are obtained by matching and analyzing the Blasingame decline curves of well A1.

6. Conclusions

This study investigates the Blasingame production decline type curves for a vertical well in water influx/waterflood reservoirs, analyses the behavior of production decline type curves, and discusses the effects of the relevant parameters on type curves. Based on the results obtained in this work, the following conclusions can be made:

(1) The production decline type curve analysis model for a vertical well in natural water influx/waterflood reservoirs is established.

(2) The Blasingame production decline curves for a vertical well in natural water influx/waterflood reservoirs are generated and divided into the four regimes: early unsteady flow regime, primary depletion flow regime, second unsteady flow regime, and system pseudosteady flow regime.

(3) The production decline type curves are affected by the natural water influx/waterflood significantly. The dimensionless maximum water influx has a significant effect on the second unsteady flow regime and system pseudosteady flow regime, and the dimensionless water influx time has mainly affected the emerging time of the second unsteady flow regime.

(4) The validation of the field case demonstrates that the Blasingame production decline type curves for water influx/waterflood boundary proposed in this study could be applied to evaluate the water influx and the time of the water influx. In other words, the work provides very meaningful references for reservoir engineers working on the dynamic analysis of the natural water influx/waterflood reservoir by matching the developed type curves with the actual field data.

Data Availability

The data used to support the findings of this study are available from the corresponding author upon request.

Disclosure

Mingqiang Wei and Yonggang Duan are both corresponding authors.

Conflicts of Interest

The authors declare that they have no conflicts of interest.

Acknowledgments

This article was supported by scientific research starting project of SWPU (No. 2018QHZ001). The authors would like to thank the Interpore 10th Annual Meeting and Jubilee to give a presentation of the manuscript.

References

[1] C. Ou, C. Li, and Z. Ma, "3D modeling of gas/water distribution in water-bearing carbonate gas reservoirs: the Longwangmiao gas field, China," *Journal of Geophysics and Engineering*, vol. 13, no. 5, pp. 745–757, 2016.

[2] X. Zhao and I. Ershaghi, "Production geology as a tool for monitoring water influx in a compartmentalized California monterey fractured reservoir," in *Proceedings of the SPE Western Regional Meeting*, pp. 23–26, Anchorage, AK, USA, May 2016.

[3] G. Gao, W. Gang, G. Zhang et al., "Physical simulation of gas reservoir formation in the Liwan 3-1 deep-water gas field in the Baiyun sag, Pearl River Mouth Basin," *Natural Gas Industry B*, vol. 2, no. 1, pp. 77–87, 2015.

[4] A. F. Van Everdingen and W. Hurst, "The application of the Laplace transformation to flow problems in reservoirs," *Journal of Petroleum Technology*, vol. 1, no. 12, pp. 305–324, 1949.

[5] M. J. Fetkovich, "A simplified approach to water influx calculations-finite aquifer systems," *Journal of Petroleum Technology*, vol. 23, no. 7, pp. 814–828, 1971.

[6] R. D. Carter and G. W. Tracy, "An improved method for calculating water influx," *SPE General*, vol. 219, pp. 415–417, 1960.

[7] D. R. Allard and S. M. Chen, "Calculation of water influx for bottomwater drive reservoirs," *SPE Reservoir Engineering*, vol. 3, no. 2, pp. 369–379, 1988.

[8] W. F. Leung, "A fast convolution method for implementing single-porosity finite/infinite aquifer models for water-influx calculations," *SPE Reservoir Engineering*, vol. 1, no. 5, pp. 490–510, 1986.

[9] W.-j. Shen, X.-h. Liu, X.-z. Li, and J.-l. Lu, "Water coning mechanism in Tarim fractured sandstone gas reservoirs," *Journal of Central South University*, vol. 22, no. 1, pp. 344–349, 2015.

[10] W. Shen, Y. Xu, X. Li, W. Huang, and J. Gu, "Numerical simulation of gas and water flow mechanism in hydraulically fractured shale gas reservoirs," *Journal of Natural Gas Science and Engineering*, vol. 35, pp. 726–735, 2016.

[11] J. B. Gu and O. V. Trevisan, "Classic models of calculation of influx: a comparative study," in *Proceedings of the Latin American & Caribbean Petroleum Engineering Conference*, Buenos Aires, Argentina, April 2007.

[12] C. Cui and X. Zhao, "Method for calculating production indices of multilayer water drive reservoirs," *Journal of Petroleum Science and Engineering*, vol. 75, no. 1-2, pp. 66–70, 2010.

[13] J. E. Omeke, A. Nwachukwu, R. O. Awo, O. Boniface, and I. N. Uche, "A new approach to aquifer influx calculation for finite aquifer system," in *Proceedings of the Nigeria Annual International Conference and Exhibition*, Abuja, Nigeria, August 2011.

[14] Y. Li, C. Jia, H. Peng, B. Li, Z. Liu, and Q. Wang, "Method of water influx identification and prediction for a fractured-vuggy carbonate reservoir," in *Proceedings of the SPE Middle East Oil & Gas Show and Conference*, Manama, Kingdom of Bahrain, March 2017.

[15] M. Dejam, H. Hassanzadeh, and Z. Chen, "Shear dispersion in combined pressure-driven and electro-osmotic flows in a channel with porous walls," *Chemical Engineering Science*, vol. 137, pp. 205–215, 2015.

[16] M. Dejam, H. Hassanzadeh, and Z. Chen, "Semi-analytical solutions for a partially penetrated well with wellbore storage and skin effects in a double-porosity system with a gas cap," *Transport in Porous Media*, vol. 100, no. 2, pp. 159–192, 2013.

[17] V. Mashayekhizadeh, M. Dejam, and M. H. Ghazanfari, "The application of numerical Laplace inversion methods for type curve development in well testing: a comparative study," *Petroleum Science and Technology*, vol. 29, no. 1, pp. 695–707, 2011.

[18] J. J. Arps, "Analysis of decline curves," *Transactions of the AIME*, vol. 160, no. 1, pp. 228–247, 1945.

[19] Y. Cheng, J. W. Lee, and D. A. Mcvay, "Quantification of uncertainty in reserve estimation from decline curve analysis of production data for unconventional reservoirs," *Journal of Energy Resources Technology*, vol. 130, no. 4, pp. 885–893, 2007.

[20] Y. Jiang and A. Dahi-Taleghani, "Modified extended finite element methods for gas flow in fractured reservoirs: a pseudo-pressure approach," *ASME Journal of Energy Resources Technology*, vol. 140, no. 7, article 073101, 2018.

[21] J. C. Palacio and T. A. Blasingame, "Decline-curve analysis using type curves-analysis of gas well production data," in *Proceedings of the SPE Rocky Mountain Regional, Low Permeability Reservoirs Symposium*, pp. 26–28, Denver, CO, USA, April 1993.

[22] M. Wei, Y. Duan, M. Dong, Q. Fang, and M. Dejam, "Blasingame decline type curves with material balance pseudo-time modified for multi-fractured horizontal wells in shale gas reservoirs," *Journal of Natural Gas Science and Engineering*, vol. 31, pp. 340–350, 2016.

[23] M. Wei, Y. Duan, M. Dong, Q. Fang, and M. Dejam, "Transient production decline behavior analysis for a multi-fractured horizontal well with discrete fracture networks in shale gas reservoirs," *Journal of Porous Media*, vol. 22, no. 3, pp. 343–361, 2019.

[24] M. Y. Shih and T. A. Blasingame, "Decline curve analysis using type curves: horizontal wells," in *Proceedings of the Joint Rocky Mountain Regional/Low Permeability Reservoirs Symposium*, Denver, CO, USA, 1995.

[25] C. R. Clarkson, C. L. Jordan, D. Ilk, and T. A. Blasingame, "Production data analysis of fractured and horizontal CBM wells," in *Proceedings of the SPE Eastern Regional Meeting*, pp. 23–25, Charleston, WV, USA, September 2009.

[26] R.-S. Nie, Y.-F. Meng, J.-C. Guo, and Y. L. Jia, "Modeling transient flow behavior of a horizontal well in a coal seam," *International Journal of Coal Geology*, vol. 92, pp. 54–68, 2012.

[27] R.-S. Nie, Y.-F. Meng, Y.-L. Jia, F.-X. Zhang, X.-T. Yang, and X.-N. Niu, "Dual porosity and dual permeability modeling of horizontal well in naturally fractured reservoir," *Transport in Porous Media*, vol. 92, no. 1, pp. 213–235, 2011.

[28] T. H. Kim, K. Park, and K. S. Lee, "Type curves for analyzing production from horizontal wells with multiple hydraulic fractures in shale gas reservoirs," in *Proceedings of the Twenty-fourth International Ocean and Polar Engineering Conferene*, Busan, Korea, June 2014.

[29] L. E. Doublet and T. A. Blasingame, "Decline curve analysis using type curves: water influx/waterflood cases," *SPE Formation Evaluation*, vol. 04, pp. 637–656, 1995.

[30] T. Marhaendrajana and T. A. Blasingame, "Decline-curve analysis using type curves devaluation of well performance behavior in a multiwell reservoir," in *Proceedings of the SPE Annual Technical Conference and Exhibition*, New Orleans, LA, USA, October 2001.

[31] H. Hassanzadeh and M. Pooladi-Darvish, "Comparison of different numerical Laplace inversion methods for engineering applications," *Applied Mathematics and Computation*, vol. 189, no. 2, pp. 1966–1981, 2007.

[32] M. Dejam and H. Hassanzadeh, "Diffusive leakage of brine from aquifers during CO_2 geological storage," *Advances in Water Resources*, vol. 111, pp. 36–57, 2018.

[33] M. Dejam, H. Hassanzadeh, and Z. Chen, "A reduced-order model for chemical species transport in a tube with a constant wall concentration," *The Canadian Journal of Chemical Engineering*, vol. 96, no. 1, pp. 307–316, 2018.

[34] H. Stehfest, "Algorithm 368: numerical inversion of Laplace transforms [D5]," *Communications of the ACM*, vol. 13, no. 1, pp. 47–49, 1970.